ESRF	**Experiment title:** Electronic and magnetic structure of SrIrO3/LaCoO3 superlattices	**Experiment number**: HC-5007
Beamline: ID12	**Date of experiment**: from: 31.01.2023 to: 07.02.2023	**Date of report**: 10.03.2023
Shifts: 18	**Local contact(s)**: Andrei Rogalev and Fabrice Wilhelm	*Received at ESRF:*

Names and affiliations of applicants (* indicates experimentalists):

Fuchs, Dirk* (Karlsruhe Institute of Technology, IQMT)
Jaiswal, Arun Kumar* (Karlsruhe Institute of Technology, IQMT)
Haghighirad, Amir-Abbas* (Karlsruhe Institute of Technology, IQMT)
Le Tacon, Matthieu (Karlsruhe Institute of Technology, IQMT)

Report:

The proximity-induced ferromagnetism in SrIrO3(SIO)/LaCoO3(LCO) heterostructures (HSs) has been demonstrated to arise from interfacial charge transfer from Ir to Co, which we here investigated in more detail using Ir L- edge x-ray absorption spectroscopy (XAS) and x-ray magnetic circular dichroism (XMCD) at beam line ID12 on a selection of high quality SIO/LCO HSs. We specifically investigated the local electronic and magnetic structure of interfacial Ir ions, and in particular checked possible break-down of the pseudo-spin scenario. We could successfully use the allocated 18 shifts to carry out XAS and XMCD at the Ir $L_{2,3}$ edge of 7 different SIO/LCO, (S*n*L*m*)x*N*, and one SIO/LaFeO3(LFO), (S*n*F*m*)x*N*, HSs. Here, *n* and *m* indicate the number of monolayers of SIO and LCO or LFO, used for the HSs and x*N* the number of repetitions to end up in a total film thickness of about 15 – 20 nm. Films were grown on SrTiO3 (001) substrates with surface area of 5 mm × 5 mm. All the measurements were carried out at T = 20 K in grazing beam incidence (15°) using the HU-38 undulator and a fluorescence detector. XMCD measurements were recorded for $B = \pm$ 6T applied in the film plane.

In Fig. 1 we have shown the Ir $L_{2,3}$ XANES spectra for all the HSs. The Ir L_3 spectrum was obtained by averaging 20 – 40 single scans, whereas for the L_2 edge spectrum 8 – 12 scans were averaged. The spectra were normalized between zero before the absorption edge and one above the edge. The most striking characteristic

of the Ir $L_{2,3}$ XANES spectra is the sharp 'white-line' (WL) feature that corresponds to $2p \rightarrow 5d$ electronic transitions.

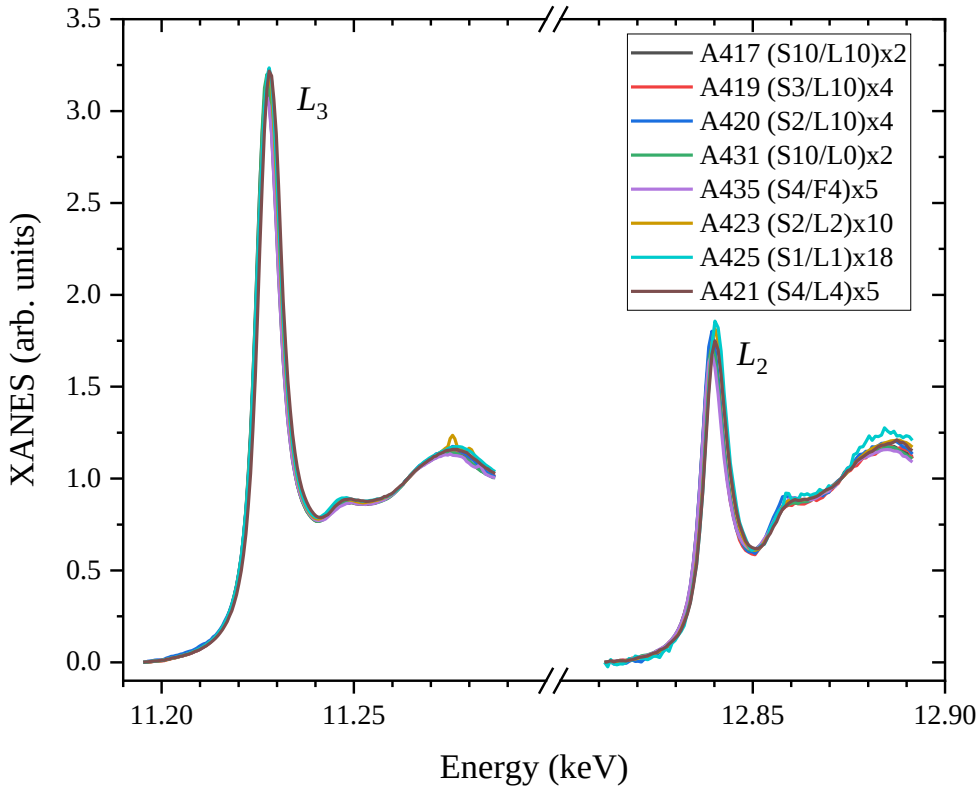

FIG. 1. Normalized intensity of the Ir L_3 and L_2 XANES (I_{L3}^{XAS} and I_{L2}^{XAS}). Measurements were taken in grazing beam incidence (15°) at T = 20 K.

The Ir L_2-edge is sensitive to transitions involving $5d_{3/2}$ (*i.e.* J_{eff} =3/2) holes, while the L_3-edge is related to both $5d_{5/2}$ (J_{eff} =1/2 and the crystal field e_g manifolds) and $5d_{3/2}$ final states. Because the WL features are more pronounced at the L_3 edge than the L_2 edge, we can infer that these unoccupied $5d$ states are primarily $5d_{5/2}$ rather than $5d_{3/2}$ in nature, consistent with the almost completely filled J_{eff} =3/2 bands.
The $L_{2,3}$ spectra display a systematic shift of spectral weight to higher energy and an increase of WL-Peak area with decreasing SIO layer thickness or number of SIO/LCO interfaces per film. This indicates an increase of the t_{2g}-derived unoccupied density of states which is very likely related to an electron transfer from Ir $5d$ to Co $3d$ states at the interface. The charge transfer inherently results in a change of the chemical valence state of Ir. In Fig. 2 we have plotted the sum of the WL-peak area, $I_{L3}^{XAS}+I_{L2}^{XAS}$, versus the SIO layer thickness. The WL-peak area was extracted by careful subtraction of the background using an arctangent background function. The position of the step-function describing transitions into the continuum was defined by the following procedure [1]. The maximum of the L_3 WL was assigned to zero energy and the L_2 edge spectrum was shifted in energy to have the first EXAFS oscillations perfectly overlapping for the two spectra. The step function was placed by visual

comparison of the shifted spectra. A step function broadening of about 6 eV was used. Further, the WL integral at the L_2 edge was divided by 2.15 reflecting factors of (i) 2 from the occupation ratios of $2p_{3/2}$ and $2p_{1/2}$ core states and (ii) 0.15 from the fact that the sum rules are applied to the line intensities and not to the absorption cross sections. The right scale of Fig. 2 indicates the corresponding chemical valence state of Ir when for the SIO single layer film (S20L0) an Ir^{4+} state is assumed. In the extreme case, where the SIO layer thickness is only one ML (S1L1), a valence state of $Ir^{4.4+}$ is deduced indicating an electron transfer of nearly half an electron per ML. Changes of the chemical valence state are usually also manifested in an energy shift of the spectral weight of the XANES. In Fig. 3 we have plotted the Ir L_3 WL-peak shift of the HSs (with respect to sample S20L0) versus the mean chemical valence state of Ir. The energy shift is nearly linear (~1.5 eV/electron) and about 2-3 times smaller compared to 3*d* transition metal oxides [2].

The effect of spin orbit coupling (SOC) on the 5*d* states was quantified through the branching ratio (BR) of the WL integrals at the SO split absorption edges for the *p* → *d* transitions: BR = $I_{L3}^{XAS}/(I_{L3}^{XAS}+I_{L2}^{XAS})$. In Tab.1 we have listed the BR and the $I_{L3}^{XAS}/I_{L2}^{XAS}$ ratio for the various HSs. The BR values are only slightly smaller compared to that of Sr2IrO4 (0.87) [3], indicating nearly pure pseudospin J_{eff} =1/2 state for all the HSs.

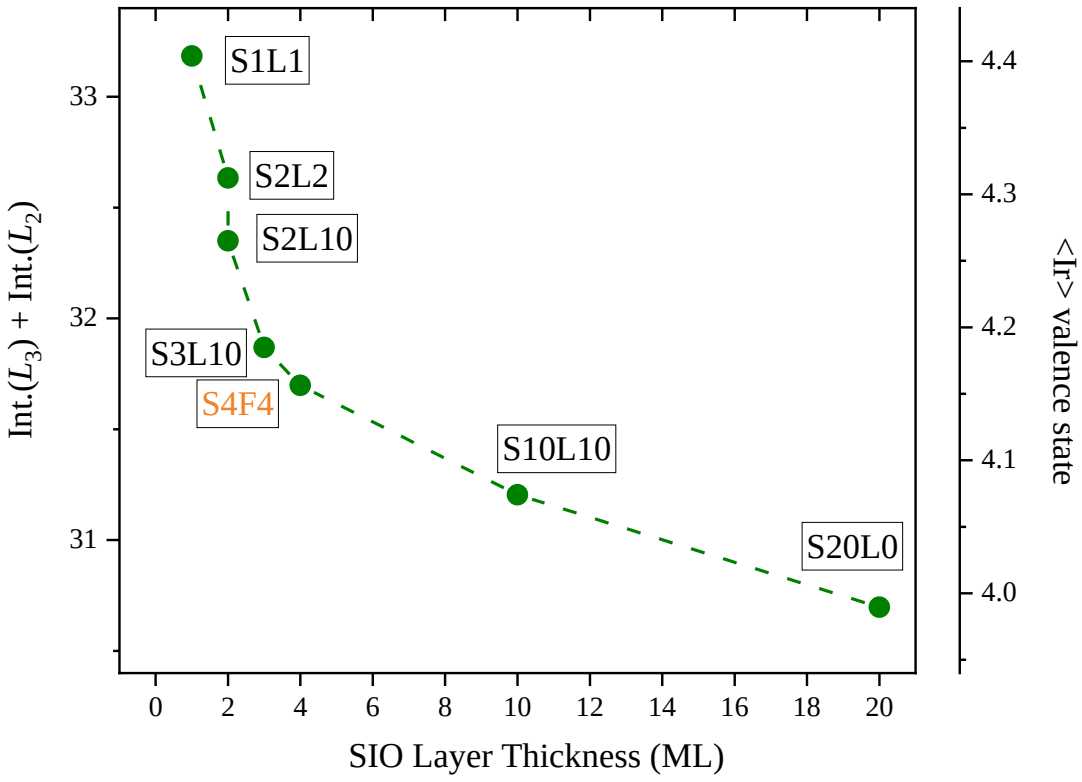

FIG. 2. Sum of the white-line peak area, $I_{L3}^{XAS}+I_{L2}^{XAS}$, obtained from the normalized Ir L_3 and L_2 XANES as a function of the SIO single layer thickness of the S*n*L*m* and S*n*F*m* heterostructures. The corresponding mean chemical valence state of Ir is shown on the right scale.

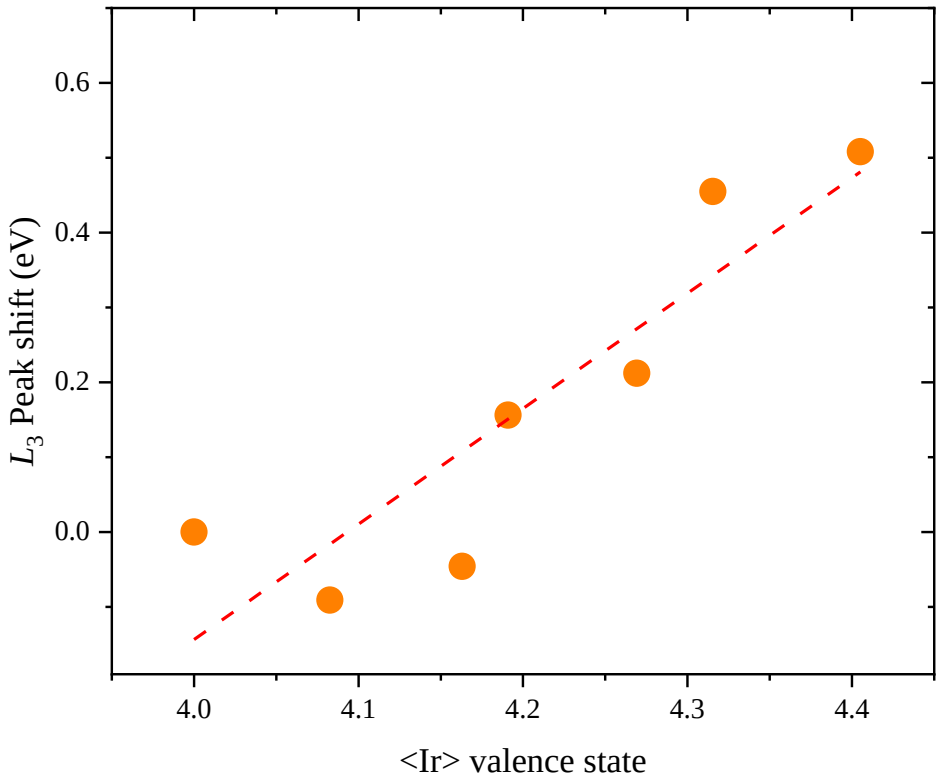

FIG. 3. Shift of the Ir L_3 WL-Peak position (chemical shift) of the heterostructures versus their mean Ir valence state.

XMCD spectra were obtained as the difference of consecutive XAS spectra obtained with different photon helicities. The spectra were recorded in both field directions (± 6T) to exclude experimental artefacts. In Fig. 4 we have shown the L_3 and L_2 XMCD signal exemplarily for two SIO/LCO HSs in comparison to that of the SIO/LFO HSs. The L_3 XMCD is rather weak and even much smaller for the L_2 edge. Note, the L_2/L_3 XMCD intensity ratio for Sr2IrO3 is only about 5% [4]. Generally, XMCD signal increases with decreasing SIO layer thickness and indicates alignment of the Ir magnetic moment parallel to the field direction, similar to the Co magnetic moment in LCO which has been analyzed in previous experiments. Hence, spin alignment in the SIO layer is parallel to that of the LCO layer documenting a FM coupling at the SIO/LCO interface. Interestingly, the Ir moment in the SIO/LFO HS (S4F4) is well comparable to that of the corresponding SIO/LCO HS (S4/L4) despite the much larger effective moment in LFO (≈ 4 μB) compared to that of LCO (≈ 0.5μB). The field dependence of the L_3 XMCD is shown in the inset of Fig. 4 for sample (S1/L1). Within the experimental resolution, no clear indication of hysteretic behavior was observed.

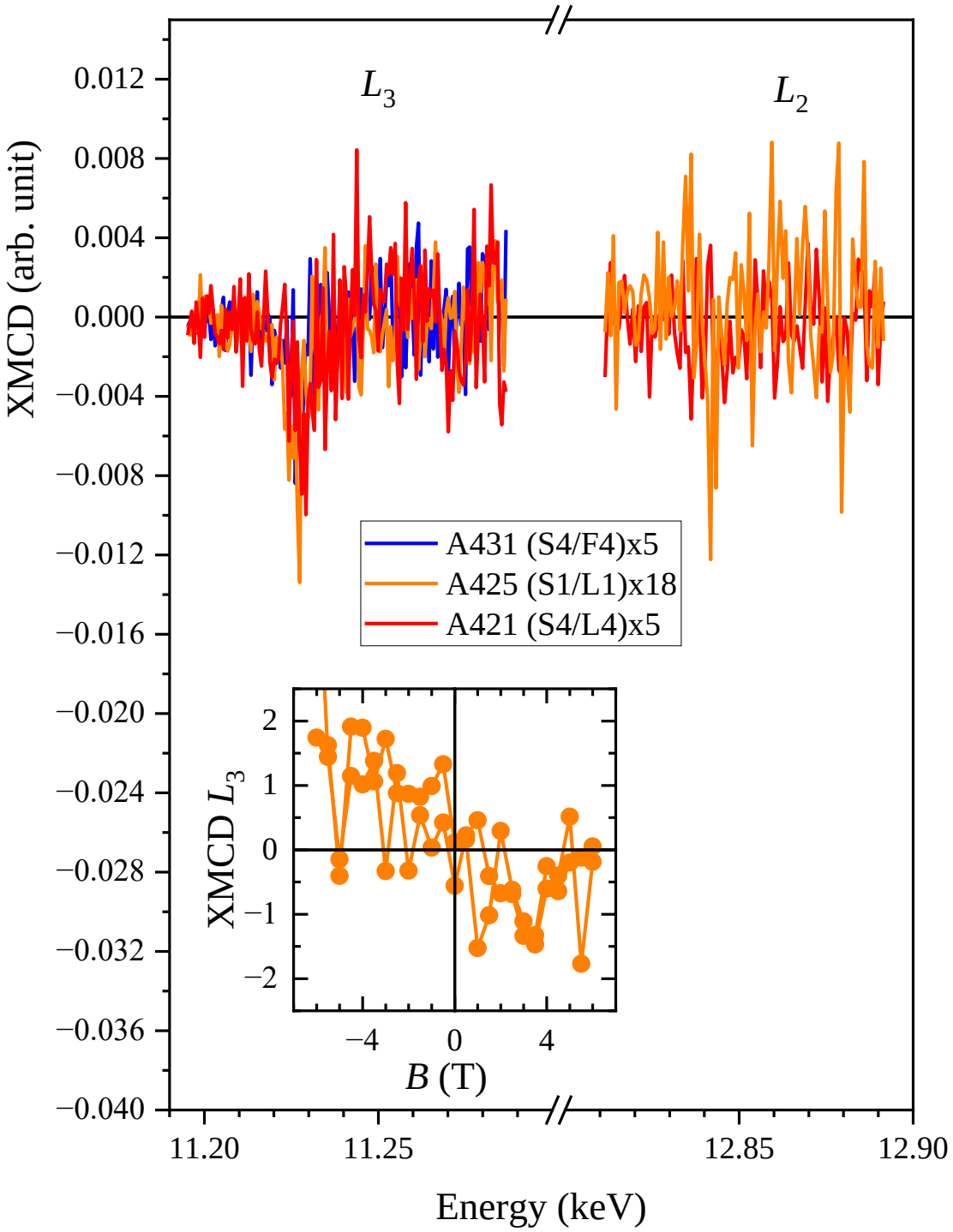

FIG. 4. Normalized XMCD at the Ir L_3 and L_2 edge. Measure-ments were taken in grazing beam incidence (15°) at T = 20 K for left and right polarized light at B = ± 6 T. Spectra are shown for the heterostructures S1L1, S4L4, and S4F4. The inset shows the magnetic field dependence of the L_3 XMCD signal at 20 K for sample S1L1.

The normalized XMCD spectra were further analyzed using the magneto-optical sum rules given by the equations for the L_2 and L_3 absorption edges for the spin- and

orbital momentum operator [5]: $s_z=n_h/2\cdot(I_{L3}^{XMCD}+I_{L2}^{XMCD})/(I_{L3}^{XAS}+I_{L2}^{XAS})$ and $l_z=2n_h/3\cdot(I_{L3}^{XMCD}-2\cdot I_{L2}^{XMCD})/(I_{L3}^{XAS}+I_{L2}^{XAS})$. The number of holes n_h was deduced from the sum of the WL integral intensities $I_{L3}^{XAS}+I_{L2}^{XAS}$ and the L_2 XMCD signal (I_{L2}^{XMCD}) was negelgted. The effective spin, orbital- and total magnetic moments are calculated by: $m_l = -l_z$, $m_s = -2s_z$, and $m_t = m_s+m_l$. As expected from the rather small L_3 XMCD signal, m_s of the HSs is quite small. Interestingly, the orbital moment m_l is even smaller despite the observed BR which indicates an SOC dominated ground state where m_l is expected to be distinct larger compared to m_s [1]. Possibly, this might be related to the difficulties in an accurate determination of the L_2 XMCD signal.

In summary, during the allocated beamtime we succesfully could adress to all the points raised in our proposal HC5007. A systematic change of the chemical valence state of Ir was observed with decreasing SIO layer thickness due to the interfacial charge transfer at the SIO/LCO interface. Despite the large degree of epitaxial strain within the HSs, the observed BR was found to be nearly the same in all HSs indicating a SO coupled pseudospin ground state of the Ir. The Ir magnetic moment was found to be rather small, $m_t \approx 0.018$ μB, and parallel alligned with respect to the magnetic field demonstrating a FM coupling of the SIO and LCO layer at the interface.

TABLE 1. Summary of the measured samples, type of the multilayer and corresponding thickness of the SIO single layer t_{SIO}. Branching ratio BR and ratio of the normalized integrated intensity $I_{L3}^{XAS}/I_{L2}^{XAS}$ as obtained from the normalized Ir L_3,L_2 XANES. The orbital-, spin-, and total moment of the Ir ion for selected eterostructures as deduced from the Ir L_3,L_2 XMCD signal. All data were taken at T = 20 K.

Sample	multilayer	t_{SIO} (ML)	BR	$I_{L3}^{XAS}/I_{L2}^{XAS}$	m_l (μB)	m_s(μB)	m_t(μB)
A435	S20L0	20	0.843	5.372			
A417	S10L10	10	0.843	5.389			
A419	S3L10	3	0.837	5.168			
A420	S2L10	2	0.839	5.234			
A423	S2L2	2	0.844	5.418	0.00709	0.0106	0.0177
A425	S1L1	1	0.846	5.495	0.00759	0.0113	0.0189
A431	S4F4	4	0.844	5.417	0.00842	0.0126	0.0210
A421	S2L4	4	0.841	5.310			

References:

[1] K. S. Pedersen et al., Nat. Commun. 7:12195 (2016).
[2] J. Garcia, J. Synchrotron Rad. 17, 386 (2010).
[3] J. P. Clancy et al., Phys. Rev. B 86, 195131 (2012).
[4] D. Haskel et al., Phys. Rev. Lett. 109, 027204 (2012).
[5] B. T. Thole et al., Phys. Rev. Lett. 68, 1943 (1992).